arranged in approximately horizontal rows, the distance between two rows being roughly equal to the wavelength of the modulated wave. This is due to the contribution of diffraction streaks, although these streaks cannot be distinguished from the noisy optical diffraction pattern. The image contrast is in agreement with the conclusion from the electron diffraction analysis and implies that the Ba-ion strings are incoherent to one another. The Ba ions with their idealized positions in the same plane parallel to the *ab* plane have different degrees of displacement along the *c* axis. In other words, the initial phases of the modulated waves spreading along the different atomic columns of Ba are different. Fig. 6(*b*) shows schematically the random phase shift of the modulated waves propagating along different tetragonal channels.

7. Effect of electron-beam irradiation

Fig. 7(*a*) is a high-resolution image taken along the [$10\bar{2}$] direction and Fig. 7(*b*) is a local image magnified from Fig. 7(*a*); Figs. 7(*c*) and 7(*d*) are the corresponding EDP and ODP, respectively. The white dots in Figs. 7(*a*) and 7(*b*) are arranged almost periodically, but in fact there is no translational periodicity at all if the intensity of the white dots is taken into consideration. In the corresponding ODP shown in Fig. 7(*d*), besides the main diffraction spots the satellite spot $\bar{1}0\bar{1}1$ (indicated by an arrow) and the satellite spot $101\bar{1}$ can be seen clearly but the modulation contrast cannot be seen. This can also be interpreted in terms of the incoherency among different atomic columns of Ba. In any case, owing to the contribution of the satellite spots, including spots $\bar{1}0\bar{1}1$ and $101\bar{1}$, the image only shows a rough periodicity along the vertical direction. The vertical intensity change of the dots located in the same horizontal line is not synchronous.

After strong electron-beam irradiation, the images taken along the [$10\bar{2}$] direction and the corresponding electron and optical diffraction patterns are shown in Fig. 8. There are no evident differences between corresponding main diffraction spots in Figs. 7(*c*) and 8(*c*), but the intensity of the satellite spots decreases greatly in Fig. 8(*c*). In Fig. 8(*b*) the white dots become more ordered in comparison with Fig. 7(*b*). This indicates that under electron-beam irradiation the incommensurate structure of ankangite tends towards a commensurate structure.

References

AXE, J. D. (1980). *Phys. Rev. B*, **21**, 4181–4190.
BEYELER, H. U. (1976). *Phys. Rev. Lett.* **37**, 1557–1560.
BURSILL, L. A. & GRZINIC, G. (1980). *Acta Cryst.* B**36**, 2902–2913.
BYSTROM, A. & BYSTROM, A. M. (1950). *Acta Cryst.* **3**, 146–154.
BYSTROM, A. & BYSTROM, A. M. (1951). *Acta Cryst.* **4**, 469.
DRYDEN, J. S. & WADSLEY, A. D. (1958). *Trans. Faraday Soc.* **54**, 1574–1580.
POST, J. E. & BURNHAM, C. W. (1986). *Am. Mineral.* **71**, 1178–1185.
POST, J. E., VON DREELE, R. B. & BUSECK, P. R. (1982). *Acta Cryst.* B**38**, 1056–1065.
SINCLAIR, W., MCLAUGHLIN, G. M. & RINGWOOD, A. E. (1980). *Acta Cryst.* B**36**, 2913–2918.
STEEDS, J. W., BIRD, D. M., EAGLESHAM, D. J., MCKERNAN, S., VINCENT, R. & WITHERS, R. (1985). *Ultramicroscopy*, **18**, 97–130.
WOLFF, P. M. DE (1974). *Acta Cryst.* A**30**, 777–785.
ZHOU, J. & MA, Z. S. (1987). *Geoscience*, **1**, 77–83.

Acta Cryst. (1990). B**46**, 117–125

Coincidence Orientations of Crystals in Tetragonal Systems, with Applications to $YBa_2Cu_3O_{7-\delta}$

BY A. SINGH, N. CHANDRASEKHAR AND A. H. KING

Department of Materials Science and Engineering, State University of New York at Stony Brook, Stony Brook, NY 11794-2275, *USA*

(*Received* 10 *April* 1989; *accepted* 21 *September* 1989)

Abstract

We have developed a method for the characterization of coincidence-site lattices (CSL's) in tetragonal or near-tetragonal orthorhombic structures, by suitable modifications to the method of Grimmer & Warrington [*Acta Cryst.* (1987), A**43**, 232–243]. We have applied our method to determine coincidence rotations and the associated information appropriate for forming constrained CSL's in the high-T_c superconductor $YBa_2Cu_3O_{7-\delta}$. The unit cell is orthorhombic with lattice parameters $a = 3{\cdot}82$, $b = 3{\cdot}89$

0108-7681/90/020117-09$03.00

and $c = 11{\cdot}67$ Å for the nominal composition. We present tables of coincidence rotation angles, Σ, CSL, DSCL and associated step vectors up to $\Sigma = 50$. We find our results to be reasonable, and representative of grain-boundary structure in $YBa_2Cu_3O_{7-\delta}$ in view of observations of grain-boundary dislocation networks in this material.

Introduction

Coincidence-site lattices (CSL's) are geometrical models of grain-boundary structure and are formed by relative rotations of two congruent lattices, using a lattice site as the origin. The ratio of the unit-cell volume of the CSL to that of the original lattice is usually denoted by Σ. The displacement-shift-complete lattice (DSCL), which is a lattice of vectors representing the displacements of one crystal with respect to the other that leaves the boundary structure shifted but complete, is also of importance in defining grain-boundary geometry. If the relative orientation between two grains deviates by only a few degrees from a coincidence orientation with a low value of Σ, then it has often been observed that the deviation from exact coincidence is accommodated by arrays of dislocations in the boundary. Small deviations from the axial ratios needed to form the CSL are accommodated in the same way, for non-cubic materials, as demonstrated by Chen & King (1988). The Burgers vectors of such grain-boundary dislocations are often vectors of the DSCL.

Another important geometrical feature besides the usual CSL and DSCL is the step vector associated with a DSC dislocation. The step vector is used in determining the height of the step in the grain boundary that is associated with the core of a grain-boundary dislocation. The definition of the step vector and an extensive description of its properties was given by King & Smith (1980) and King (1982). Step vectors for grain-boundary dislocations in cubic materials were tabulated by King (1982) and for h.c.p. materials by Chen & King (1987).

Interest in the structure and behaviour of grain boundaries in $YBa_2Cu_3O_{7-\delta}$ is increasing due to the problems of achieving sufficiently high critical current densities in polycrystalline samples. Knowledge of the possible geometries of coincidence-related grain boundaries is therefore essential, and in this paper we indicate appropriate techniques for the determination of such information, and provide tabulations of such data. Although $YBa_2Cu_3O_{7-\delta}$ is orthorhombic, it is very closely approximated by a tetragonal unit cell. We presume that coincidences of the tetragonal lattices can form the basis for 'constrained-coincidence' structures in $YBa_2Cu_3O_{7-\delta}$.

General theory for tetragonal structures

(a) The rotational matrix

We follow the development given by Grimmer & Warrington (1987) for hexagonal lattices. In the case of tetragonal crystals we find the following.

The crystal basis $\mathbf{e}$ consisting of three mutually orthogonal vectors $\mathbf{e}_1$, $\mathbf{e}_2$, $\mathbf{e}_3$ of lengths a, a and $c = \rho a$, is related to the cubic basis $\boldsymbol{\varepsilon}$ consisting of three mutually orthogonal vectors, each of length a, by $\mathbf{e} = \boldsymbol{\varepsilon} S$, where

$$S = \begin{pmatrix} 1 & 0 & 0 \\ 0 & 1 & 0 \\ 0 & 0 & \rho \end{pmatrix}. \tag{1}$$

Consider a right-handed rotation by an angle $\theta = 2\varphi$, $0 \le \theta \le \pi$, about an axis with cubic components ν satisfying $\nu_1^2 + \nu_2^2 + \nu_3^2 = 1$, with parameters

$$[\alpha, \beta, \gamma, \delta] = [\cos\varphi, \nu_1\sin\varphi, \nu_2\sin\varphi, \nu_3\sin\varphi]. \tag{2}$$

The general form of the rotation matrix in cubic coordinates for the rotation considered above may be found in Grimmer & Warrington (1987). The crystal components n of the rotation axis are given by:

$$\mathbf{e}n = \boldsymbol{\varepsilon}Sn = \boldsymbol{\varepsilon}\nu$$

i.e.

$$\nu = Sn$$

$$\nu_l = n_1, \quad \nu_2 = n_2, \quad \nu_3 = \rho n_3$$

and

$$1 = \nu_1^2 + \nu_2^2 + \nu_3^2 = n_1^2 + n_2^2 + \rho^2 n_3^2. \tag{3}$$

Introducing parameters:

$$(A, B, C, D) = \pm(\cos\varphi, n_1\rho\sin\varphi, n_2\rho\sin\varphi, n_3\rho\sin\varphi), \tag{4}$$

we obtain from (2) and (3),

$$[\alpha, \beta, \gamma, \delta] = \pm[A, B/\rho, C/\rho, D]. \tag{5}$$

The modified rotation matrix for tetragonal structures takes the form

$$R_0 = \begin{bmatrix} A^2 - D^2 + \tau(B^2 - C^2) & 2(BC\tau - AD) & 2\sqrt{\tau}(BD + AC) \\ 2(BC\tau + AD) & A^2 - D^2 - \tau(B^2 - C^2) & 2\sqrt{\tau}(CD - AB) \\ 2\sqrt{\tau}(BD - AC) & 2\sqrt{\tau}(CD + AB) & A^2 + D^2 - \tau(B^2 + C^2) \end{bmatrix}, \tag{6}$$

where

$$\tau = 1/\rho^2. \tag{7}$$

Using (3) and (4), the normalization condition satisfied by the parameters (A, B, C, D) is:

$$A^2 + D^2 + \tau(B^2 + C^2) = \cos^2\varphi + \sin^2\varphi(n_1^2 + n_2^2 + \rho^2 n_3^2) = 1. \tag{8}$$

Expressing the original and rotated vectors in the basis $\mathbf{e}$ we obtain

$$\boldsymbol{\varepsilon}\xi = \mathbf{e}S^{-1}\xi = \mathbf{e}x$$

and $\boldsymbol{\varepsilon}\xi' = \boldsymbol{\varepsilon}R_0\xi = \mathbf{e}S^{-1}R_0Sx$ where $x = S^{-1}\xi$ and $R = S^{-1}R_0S$, *i.e.*

$$R = \begin{bmatrix} A^2 - D^2 + \tau(B^2 - C^2) & 2(BC\tau - AD) & 2(BD + AC) \\ 2(BC\tau + AD) & A^2 - D^2 - \tau(B^2 - C^2) & 2(CD - AB) \\ 2\tau(BD - AC) & 2\tau(CD + AB) & A^2 + D^2 - \tau(B^2 + C^2) \end{bmatrix}. \quad (9)$$

(*b*) *Coincidence rotations*

A rotation will generate a three-dimensional CSL if, and only if, the matrix R in lattice coordinates is rational. From this it follows that R^{-1} is also rational. R^{-1} is obtained by replacing A by $-A$ in (9). Denoting the elements of R by R^+_{ij} and the elements of R^{-1} by R^-_{ij}, it can be deduced from (8) and (9), that the following constraints apply:

$$4A^2 = 1 + R^+_{11} + R^+_{22} + R^+_{33} \quad (10a)$$
$$4AB = R^-_{23} - R^+_{23} \quad (10b)$$
$$4AC = R^+_{13} - R^-_{13} \quad (10c)$$
$$4AD = R^-_{12} - R^+_{12} \quad (10d)$$
$$4BD = R^+_{13} + R^-_{13} \quad (10e)$$
$$4CD = R^+_{23} + R^-_{23} \quad (10f)$$
$$4D^2 = 1 - R^+_{11} - R^+_{22} + R^+_{33} \quad (10g)$$
$$4\tau B^2 = 1 + R^+_{11} - R^+_{22} - R^+_{33} \quad (10h)$$
$$4\tau BA = R^+_{32} - R^-_{32} \quad (10i)$$
$$4\tau BD = R^+_{31} + R^-_{31} \quad (10j)$$
$$4\tau BC = R^+_{21} + R^-_{21} \quad (10k)$$
$$4\tau AC = R^-_{31} - R^+_{31} \quad (10l)$$
$$4\tau DC = R^+_{32} + R^-_{32} \quad (10m)$$
$$4\tau C^2 = 1 - R^+_{11} + R^+_{22} - R^+_{33}. \quad (10n)$$

From the above set of equations it follows that coincidence rotations are possible for irrational τ only if $AB = AC = BD = CD = 0$, *i.e.* if either $A = D = 0$ or $B = C = 0$. For rational τ and for $A \neq 0$, there exists a $k \neq 0$ and four coprime integers m, U, V, W such that

$$A^2 = km, \quad AB = kU, \quad AC = kV, \quad AD = kW. \quad (11)$$

In other words

$$\text{g.c.d}(m, U, V, W) = 1. \quad (12)$$

From (11) and (12), we obtain

$$km = A^2 = A^2[A^2 + D^2 + \tau(B^2 + C^2)]$$
$$= k^2[m^2 + W^2 + \tau(U^2 + V^2)] = k^2s, \quad (13)$$

where

$$s = [m^2 + W^2 + \tau(U^2 + V^2)] \quad (14)$$

and

$$A = m/\sqrt{s}, \quad B = U/\sqrt{s}, \quad C = V/\sqrt{s}, \quad D = W/\sqrt{s}. \quad (15)$$

Using the relations (15), R transforms to

$$R = \frac{1}{s}\begin{bmatrix} m^2 - W^2 + \tau(U^2 - V^2) & 2(UV\tau - mW) & 2(UW + mV) \\ 2(UV\tau + mW) & m^2 - W^2 - \tau(U^2 - V^2) & 2(VW - mU) \\ 2\tau(UW - mV) & 2\tau(VW + mU) & m^2 + W^2 - \tau(U^2 + V^2) \end{bmatrix}, \quad (16)$$

where

$$m = W = 0 \text{ or } U = V = 0 \text{ if } \tau \text{ is irrational.} \quad (17)$$

Equations (12), (14), (16) and (17) are sufficient to guarantee that R is rational, *i.e.* R describes a coincidence rotation.

Coincidence rotations, therefore, can be denoted by quadruples (m, U, V, W) consisting of four coprime integers. The normalization condition is given by (12). The expressions for $[B, C, D]$, for the axis and $\cos\varphi = A$ for the angle, can now be written as $[U, V, W]$ and $\cos\varphi = m/\sqrt{s}$, *i.e.*

$$\cos\varphi = m/[m^2 + W^2 + \tau(U^2 + V^2)]^{1/2}$$
$$\tan\varphi = [W^2 + \tau(U^2 + V^2)]^{1/2}/m$$
$$= (n/m)[w^2 + \tau(u^2 + v^2)]^{1/2}, \quad (18)$$

where

$$n = \text{g.c.d}(U, V, W),$$
$$u = U/n, \quad v = V/n, \quad w = W/n. \quad (19)$$

From (12) and (19)

$$\text{g.c.d}(u, v, w) = 1, \quad \text{g.c.d}(m, n) = 1. \quad (20)$$

For rational τ there exist positive integers μ and ν such that:

$$\nu/\mu = \tau, \quad \text{g.c.d}(\mu, \nu) = 1. \quad (21)$$

If we set

$$F = \mu s = \mu(m^2 + W^2) + \nu(U^2 + V^2), \quad (22)$$

R becomes:

$$R = \frac{1}{F}\begin{bmatrix} \mu(m^2 - W^2) + \nu(U^2 - V^2) & 2(\nu UV - \mu mW) & 2\mu(UW + mV) \\ 2(\nu UV + \mu mW) & \mu(m^2 - W^2) - \nu(U^2 - V^2) & 2\mu(VW - mU) \\ 2\nu(UW - mV) & 2\nu(VW + mU) & \nu(m^2 + W^2) - \nu(U^2 + V^2) \end{bmatrix}. \quad (23)$$

Multiplying both sides of (10) by F and using the notation $r_{ij}^{\mp} = FR_{ij}^{\mp}$ we obtain the following relations:

$$4\mu m^2 = F + r_{11}^{+} + r_{22}^{+} + r_{33}^{+} \qquad (24a)$$
$$4\mu m U = r_{23}^{-} - r_{23}^{-} \qquad (24b)$$
$$4\mu m V = r_{13}^{+} - r_{13}^{-} \qquad (24c)$$
$$4\mu m W = r_{12}^{-} - r_{12}^{+} \qquad (24d)$$
$$4\mu UW = r_{13}^{+} + r_{13}^{-} \qquad (24e)$$
$$4\mu VW = r_{23}^{+} + r_{23}^{-} \qquad (24f)$$
$$4\mu W^2 = F - r_{11}^{+} - r_{22}^{+} + r_{33}^{+} \qquad (24g)$$
$$4\nu U^2 = F + r_{11}^{+} - r_{22}^{+} - r_{33}^{+} \qquad (24h)$$
$$4\nu m U = r_{32}^{+} - r_{32}^{-} \qquad (24i)$$
$$4\nu UW = r_{31}^{+} + r_{31}^{-} \qquad (24j)$$
$$4\nu UV = r_{21}^{+} + r_{21}^{-} \qquad (24k)$$
$$4\nu m V = r_{31}^{-} - r_{31}^{+} \qquad (24l)$$
$$4\nu VW = r_{32}^{+} + r_{32}^{-} \qquad (24m)$$
$$4\nu V^2 = F - r_{11}^{+} + r_{22}^{+} - r_{33}^{+}. \qquad (24n)$$

(*c*) *Determination of* Σ

Equation (22) for F may be written as:

$$F = \mu s = \mu(m^2 + W^2) + \nu(U^2 + V^2) = \alpha\Sigma.$$

From the set of equations (24) and Grimmer's α-hex theorem (Grimmer & Warrington 1987), it can be deduced that α is a factor of $4\mu\nu$. This can be used to obtain constraints on the values of α, m, U, V and W. Thus, we obtain the values of these parameters for which coincidence rotations can exist, and also the associated Σ values. These constraints ensure that the matrices ΣR and ΣR^{-1} are integral and indeed yield coincidence rotations.

(*d*) *Determination of bases for the CSL and the DSCL*

The modified form of the rotation matrix described above was used to determine the bases for the CSL and the DSCL by the method of Grimmer & Warrington (1987). These bases were further reformed to a Buerger cell, defined as the cell formed by the three smallest linearly independent vectors.

(*e*) *Determination of the step vectors associated with DSC dislocations*

The step vectors that are associated with the cores of the grain-boundary dislocations were determined by the method of Chen & King (1987). The step vectors are defined as:

$$\mathbf{S} = \mathrm{DSC} + R\mathbf{X}_2 \qquad (25)$$

where R is the rotation matrix and $\mathbf{X}_2$ is a lattice vector of lattice 2.

Results

We have applied the general theory developed above to the determination of the structure of the grain boundaries in the high-T_c superconductor $YBa_2Cu_3O_{7-\delta}$. (δ indicates the sub-stoichiometry of oxygen.) The lattice parameters a, b and c are found to vary with δ, and have been determined by Johnston (1987). The unit cell is orthorhombic with lattice parameters $a = 3{\cdot}82$, $b = 3{\cdot}89$ and $c = 11{\cdot}67$ Å for the nominal composition. Since it is necessary to have rational values of $a^2{:}b^2{:}c^2$ for the existence of coincidence rotations, these have been rounded to the closest rational values. This necessitates the consideration of the structure to be tetragonal. These approximations lead to so-called 'constrained-CSL' (CCSL) structures, postulated by Bonnet (1981). It is necessary to introduce the concept of constrained coincidence to accommodate the irrational axial ratios of real materials, the idea being that any small deviation from an ideal $a^2{:}b^2{:}c^2$ can be accommodated by an array of dislocations. Boundary structures related to CCSL's have been observed in h.c.p. metals by Chen & King (1988). The motivation in choosing a series of ratios in our calculations is to determine the possibility of the existence of coincidence orientations for varying δ, in the interval $a^2{:}b^2{:}c^2 = 15{:}15{:}135$ to $15{:}15{:}140$. We also consider an axial ratio of 6/55, which is obtained as $[(a+b)/2c]^2$.

Grain boundaries in this material are of considerable interest due to the problems of achieving requisite properties for various applications. Segregation at grain boundaries and grain-boundary-dislocation networks have been observed by Babcock (1988), Babcock & Larbalestier (1989) and Chisholm & Smith (1989). Transmission electron microscopy studies on the grain-boundary structure of $YBa_2Cu_3O_{7-\delta}$ are in progress, to determine whether three-dimensional CSL's are important in governing the structures of large-angle grain boundaries. The methods described herein could be applied to any tetragonal or near-tetragonal orthorhombic lattice.

Erochine & Nouet (1983) were the first to try determining coincidence rotations systematically for tetragonal lattices. It must be noted, however, that they assume $\Sigma = \Sigma'$, which is not always true.

We present our results for the axial ratio 1:1:9 in Table 1. All of the coincidence systems are characterized by the unique disorientation description, in order to prevent ambiguity. The data to be deposited comprise a comprehensive list of Σ values, axes, angles, CSL's, DSC's and step vectors for all axial

Table 1. *CSL, DSC and step vectors for near-tetragonal* $YBa_2Cu_3O_{7-\delta}$

The 'System' column gives the values of Σ, rotation axis and rotation angle (°). The rotation-matrix elements and DSC are multiplied by Σ. All vectors are to be read columnwise. The first given step vector corresponds to the first given DSC vector, *etc.*

System	ΣR	CSL	ΣDSC	Step vector
(*a*) For any $a^2:b^2(=a^2):c^2$				
Σ1 0 0 1 90·000	0 −1 0 1 0 0 0 0 1	0 −1 0 1 0 0 0 0 1	1 0 0 0 1 0 0 0 1	0 0 0 0 0 0 0 0 0
Σ5 0 0 1 36·870	4 −3 0 3 4 0 0 0 5	2 1 0 −1 2 0 0 0 1	−1 2 0 −2 −1 0 0 0 5	0 1 0 −1 0 0 0 0 0
Σ13 0 0 1 22·620	12 −5 0 5 12 0 0 0 13	−2 3 0 −3 −2 0 0 0 1	−2 3 0 −3 −2 0 0 0 13	0 −2 0 −2 0 0 0 0 0
Σ17 0 0 1 28·072	15 −8 0 8 15 0 0 0 17	4 −1 0 1 4 0 0 0 1	1 4 0 −4 1 0 0 0 17	0 −2 0 2 0 0 0 0 0
Σ25 0 0 1 16·260	24 −7 0 7 24 0 0 0 25	3 −4 0 4 3 0 0 0 1	−3 4 0 −4 −3 0 0 0 25	0 3 0 3 0 0 0 0 0
Σ29 0 0 1 43·603	21 −20 0 20 21 0 0 0 29	5 −2 0 2 5 0 0 0 1	−5 2 0 −2 −5 0 0 0 29	2 2 0 2 −2 0 0 0 0
Σ37 0 0 1 18·925	35 −12 0 12 35 0 0 0 37	6 −1 0 1 6 0 0 0 1	1 6 0 −6 1 0 0 0 37	0 −3 0 3 0 0 0 0 0
Σ41 0 0 1 12·680	40 −9 0 9 40 0 0 0 41	4 −5 0 5 4 0 0 0 1	−4 5 0 −5 −4 0 0 0 41	0 4 0 4 0 0 0 0 0
(*b*) For $a^2:b^2:c^2$ = 1:1:9 (15:15:135)				
Σ3 1 0 0 90·000	3 0 0 0 0 −9 0 1 0	1 0 0 0 0 −3 0 1 0	3 0 0 0 3 0 0 0 1	0 0 0 0 −1 0 0 0 0
Σ5 1 0 0 36·870	5 0 0 0 4 −9 0 1 4	1 0 0 0 5 −1 0 0 1	5 0 0 0 1 4 0 −1 1	0 0 0 0 1 0 0 0 0
Σ5 1 1 1 95·739	0 −4 9 5 0 0 0 1 4	0 −5 1 1 0 0 0 0 1	4 0 1 0 5 0 −1 0 1	0 0 −1 0 0 0 0 0 0
Σ7 2 1 0 73·398	6 2 9 2 3 −18 −1 2 2	0 2 1 −1 1 −3 −1 0 0	7 −1 1 0 2 5 0 −1 1	1 1 1 0 0 0 0 0 0
Σ9 1 1 0 70·529	6 3 18 3 6 −18 −2 2 3	−2 1 3 1 1 −3 −1 0 −1	3 −3 6 −3 3 3 −1 −2 1	1 1 1 −1 0 −1 −1 0 −1
Σ9 3 0 1 70·529	6 −6 9 6 3 −18 1 2 6	2 −1 1 1 4 −1 0 0 1	3 −6 3 3 3 3 −1 −1 2	1 0 1 1 1 1 0 0 0
Σ9 3 3 1 60·000	6 −3 18 6 6 −9 −1 2 6	−1 1 4 1 2 −1 −1 0 0	6 −3 3 −3 6 3 −1 −1 1	1 1 1 1 0 1 0 0 0
Σ11 1 1 0 50·479	9 2 18 2 9 −18 −2 2 7	−1 1 4 1 1 −5 −1 0 −1	10 −1 1 1 1 10 −1 −1 1	2 2 2 −2 −2 −2 −1 −1 −1
Σ11 9 9 1 82·163	6 2 27 7 6 −18 −2 3 2	−2 0 3 −3 −1 −1 0 −1 0	3 3 5 −2 9 4 −1 −1 2	0 0 0 −1 −1 −1 0 0 0
Σ13 1 0 0 67·380	13 0 0 0 5 −36 0 4 5	1 0 0 0 9 −2 0 2 1	13 0 0 0 2 9 0 −1 2	0 0 0 0 1 4 0 1 1
Σ13 3 3 1 92·204	4 −3 36 12 4 −9 −1 4 4	1 −3 1 0 1 4 −1 0 0	4 0 5 −1 13 2 −1 0 2	0 0 0 1 1 2 0 0 0
Σ13 9 0 1 76·658	12 −4 9 4 3 −36 1 4 4	4 −1 0 1 3 1 0 0 1	1 2 12 −4 5 4 −1 −2 1	1 2 0 0 1 0 0 0 0
Σ15 1 0 0 53·130	15 0 0 0 9 −36 0 4 9	1 0 0 0 3 6 0 −2 1	15 0 0 0 3 6 0 −2 1	0 0 0 0 2 4 0 −1 0
Σ15 9 3 1 95·739	12 0 27 9 0 −36 0 5 0	−1 0 5 3 0 0 0 1 0	−3 6 0 −6 −3 0 0 0 5	1 2 0 1 1 0 0 0 0
Σ17 1 0 0 61·928	17 0 0 0 8 −45 0 5 8	1 0 0 0 5 −7 0 1 2	17 0 0 0 2 5 0 −3 1	0 0 0 0 1 −2 0 1 1
Σ17 1 1 0 86·628	9 8 36 8 9 −36 −4 4 1	−2 1 4 2 1 −5 −1 0 −2	13 −2 4 4 2 13 −2 −1 2	2 0 2 −2 0 −2 −1 −1 −1
Σ17 3 0 1 93·372	8 −12 27 12 −1 −36 3 4 8	0 1 3 −2 3 −2 −1 −1 0	3 6 5 −4 9 −1 −1 −2 4	1 2 1 0 −1 0 −1 −1 0
Σ17 9 9 1 63·821	12 1 36 8 12 −27 −3 4 8	2 −3 −2 0 −1 3 −1 −1 0	4 −5 9 −3 8 6 −1 −3 2	−1 0 −1 0 0 1 −1 0 −1
Σ19 1 1 0 26·525	18 1 18 1 18 −18 −2 2 17	−1 1 9 0 1 −9 −1 0 −1	−1 −9 10 1 9 9 −2 1 1	1 4 4 0 −4 −4 0 −1 −1
Σ19 3 1 0 93·017	17 6 18 6 1 −54 −2 6 −1	−1 3 0 3 1 −3 −1 0 −1	18 −1 3 3 3 10 −1 −1 3	0 0 1 0 0 0 −1 −1 −1
Σ19 3 3 1 73·174	10 −6 45 15 10 −18 −2 5 10	3 2 3 −2 0 3 0 −1 1	5 −4 4 −2 13 6 −1 −3 3	3 3 2 1 0 0 0 0 0
Σ19 9 0 1 93·017	17 −6 18 6 −1 −54 2 6 1	3 −1 0 1 3 −3 0 1 1	1 3 18 −3 10 3 −1 −3 1	0 1 0 0 0 0 1 1 1
Σ19 9 0 2 71·592	15 −10 18 10 6 −45 2 5 10	0 5 2 −2 2 −3 −1 0 0	2 4 11 −5 9 1 −1 −2 4	2 2 2 1 0 0 0 0 0
Σ21 3 3 1 38·213	18 −6 27 9 18 −18 −2 3 18	−1 2 5 0 3 −3 −1 0 0	9 −3 6 −6 9 3 −1 −2 4	1 1 2 1 0 1 0 0 0
Σ21 3 3 1 81·787	9 −6 54 18 9 −18 −2 6 9	−2 1 4 0 3 −3 −1 0 −1	9 −6 3 −3 9 6 −2 −1 4	0 1 0 1 0 1 0 −1 0
Σ21 6 0 1 73·398	18 −9 18 9 6 −54 2 6 9	3 −3 0 1 4 −2 0 1 1	3 −9 12 −9 6 6 −2 −1 −1	1 0 −1 0 1 1 0 1 1
Σ23 1 0 1 55·583	14 −18 9 18 13 −18 1 2 22	2 −5 1 1 9 0 0 0 1	9 −5 −4 5 10 8 −1 −2 3	1 0 0 1 1 1 0 0 0
Σ23 1 1 1 40·459	18 −13 18 14 18 −9 −1 2 22	0 1 9 1 2 −5 −1 0 0	8 −10 5 −4 5 9 −3 −2 1	1 1 0 0 0 0 0 0 0
Σ23 3 1 0 55·583	22 3 18 3 14 −54 −2 6 13	−2 3 3 1 1 −5 −1 0 −1	−1 −10 12 3 7 10 −2 3 1	1 1 1 0 −2 −2 0 −1 −1
Σ23 9 0 1 55·583	22 −6 9 6 13 −54 1 6 14	−1 −3 2 −4 1 −2 0 −1 −1	1 3 19 −6 5 1 −1 −3 4	0 −1 −1 −1 −2 −2 0 −1 −1
Σ23 9 9 5 86·261	6 −13 54 22 6 −9 −1 6 14	2 3 4 −2 4 1 −1 −1 0	6 −5 5 −1 20 3 −1 −3 3	1 2 3 0 1 1 0 −1 −1
Σ25 1 0 0 73·740	25 0 0 0 7 −72 0 8 7	1 0 0 0 4 −9 0 1 4	25 0 0 0 9 4 0 −4 1	0 0 0 −4 −4 1 2 2 1
Σ25 2 1 1 63·896	15 −16 36 20 12 −27 0 5 20	1 −4 2 3 3 1 −1 0 1	5 10 4 −10 5 −3 0 0 5	1 1 0 2 1 2 0 0 0
Σ25 3 1 1 51·684	20 −12 27 15 16 −36 0 5 20	1 −3 3 2 4 1 −1 0 1	−5 10 3 −10 −5 −4 0 0 5	1 2 1 1 2 2 0 0 0
Σ25 9 0 4 90·000	9 −20 36 20 0 −45 4 5 16	−1 0 4 1 5 0 −1 0 −1	4 −9 8 −5 5 15 −1 −4 −2	1 0 1 1 1 2 0 0 −1
Σ25 9 9 1 51·684	20 0 45 9 20 −36 −4 5 16	−1 0 5 1 4 0 −1 1 0	5 −5 10 −4 9 12 −1 −4 3	1 1 2 1 0 2 0 0 0
Σ27 1 1 0 38·942	24 3 36 3 24 −36 −4 4 21	−2 1 6 1 1 −6 −2 0 −1	6 −3 15 −6 3 12 −1 −4 2	3 1 0 −2 0 1 −1 0 −1

Table 1 (*cont.*)

System	ΣR	CSL	ΣDSC	Step vector
Σ27 1 1 1 67·115	12 −21 36 24 12 −9 −1 4 24	−1 1 6 −1 4 −3 −1 0 0	−3 −6 12 −6 15 −3 −2 −4 −1	1 1 0 2 0 1 0 0 0
Σ27 2 1 0 96·379	21 12 36 12 3 −72 −4 8 −3	−3 2 2 6 1 −2 −2 0 −1	−3 −12 6 6 −3 15 −2 1 4	−1 1 1 3 1 0 −1 −1 0
Σ27 3 0 1 38·942	24 −12 9 12 21 −36 1 4 24	1 −3 4 1 6 1 −1 0 0	3 6 12 −12 3 6 −1 −2 5	1 2 0 0 1 1 0 0 0
Σ27 3 0 2 96·379	3 −24 36 24 −3 −36 4 4 21	1 −2 −6 1 1 6 0 −2 1	6 −3 15 −6 3 12 −1 −4 2	−3 0 −1 4 1 1 0 0 −1
Σ27 6 0 1 96·379	21 −12 36 12 −3 −72 4 8 3	2 −3 2 1 6 −2 0 2 1	3 −6 12 −6 12 3 −2 −5 1	−1 1 1 3 1 1 1 1 1
Σ27 6 3 2 90·000	12 −12 63 24 3 −36 1 8 12	5 0 −1 2 −3 2 0 −1 −1	3 −12 6 6 3 12 −2 −1 5	0 0 2 −1 −1 1 0 0 −1
Σ27 6 6 1 90·000	12 3 72 21 12 −36 −4 8 3	−2 1 6 2 2 −3 −1 0 −2	3 −6 12 12 3 −6 −1 2 5	1 3 1 1 −1 0 −1 −1 −1
Σ27 9 3 1 67·115	24 −3 36 12 12 −63 −1 8 12	−2 −3 2 1 0 5 −1 1 0	15 −6 −3 −6 −3 12 −4 −2 −1	−1 −1 −1 3 2 0 0 0 0
Σ29 1 0 0 46·397	29 0 0 0 20 −63 0 7 20	1 0 0 0 7 −8 0 1 3	29 0 0 0 1 7 0 −4 1	0 0 0 0 −2 2 0 1 1
Σ29 3 2 1 76·032	16 −12 63 24 11 −36 −1 8 16	−3 −4 −3 −2 −3 2 −1 1 0	3 6 13 −10 9 5 −2 −4 1	−3 −4 −4 −1 −1 −1 0 0 0
Σ29 5 1 1 66·637	24 −11 36 16 12 −63 1 8 16	2 −3 2 −3 −4 3 0 −1 −1	5 −10 9 13 3 6 −1 2 4	0 0 0 0 −1 −2 0 −1 −1
Σ29 9 0 2 84·062	21 −16 36 16 3 −72 4 8 11	2 −2 1 1 4 −4 0 1 2	2 8 17 −4 13 −5 −1 −4 6	−1 1 1 1 1 −1 1 0 1
Σ29 9 9 2 76·032	16 −3 72 21 16 −36 −4 8 11	−4 1 4 1 2 −2 −2 0 −1	4 −5 13 −2 17 8 −1 −6 4	1 −1 1 −1 1 1 −1 −1 0
Σ31 4 1 1 80·718	21 −14 54 22 6 −63 2 9 14	0 7 4 −2 4 −1 −1 −1 0	5 10 6 −11 9 −7 −1 −2 5	4 1 2 1 0 0 −1 0 0
Σ31 5 1 0 80·718	30 5 18 5 6 −90 −2 10 5	−3 2 3 2 3 −3 −1 −1 −1	−1 −14 17 5 8 8 −2 3 3	0 1 2 1 0 0 0 −1 −1
Σ31 5 3 1 72·154	22 −6 63 21 14 −54 −2 9 14	1 2 5 −4 0 3 0 −1 1	11 −7 9 −5 6 10 −1 −5 2	4 2 1 0 −1 0 0 0 0
Σ31 9 0 2 54·504	27 −14 18 14 18 −63 2 7 22	−1 −7 −4 1 −2 2 −1 0 1	2 6 21 −7 10 4 −1 −3 5	−3 −2 −2 −1 0 0 0 0 0
Σ31 9 9 5 72·154	14 −18 63 27 14 −18 −2 7 22	−1 −5 −2 1 −2 4 −1 0 1	7 −3 3 −2 23 8 −1 −4 4	−4 −2 −3 1 0 1 0 0 0
Σ33 3 1 1 82·163	18 −18 63 27 6 −54 2 9 18	0 6 3 −3 4 −2 −1 −1 0	6 −9 −3 9 3 12 −3 −1 7	2 3 1 0 0 0 −1 −1 0
Σ33 3 3 2 62·964	18 −21 54 27 18 −18 −2 6 27	−1 1 9 0 3 −3 −1 0 −1	9 −3 6 −3 12 9 −1 −7 3	4 3 4 −1 −1 0 −1 −1 −1
Σ33 6 3 1 62·964	27 −6 54 18 18 −63 −2 9 18	2 3 3 −3 0 3 0 −1 2	21 −3 9 3 9 6 −4 −1 3	2 3 3 0 0 0 0 1 0
Σ35 4 3 1 88·363	17 −6 90 30 10 −45 −2 11 10	4 1 4 −4 0 3 1 −1 1	−1 −9 8 −10 15 10 −4 −1 −3	3 2 3 0 −2 −1 0 0 0
Σ35 5 0 1 88·363	26 −18 45 18 1 −90 5 10 10	2 −5 1 1 10 −2 0 2 1	7 14 −2 −14 7 4 0 0 5	−1 −1 0 2 4 1 1 1 1
Σ35 5 3 0 88·363	26 15 54 15 10 −90 −6 10 1	1 4 −1 4 3 −1 −1 1 1	−3 −10 19 5 5 15 −2 5 1	2 1 1 1 1 3 0 1 0
Σ35 5 5 1 80·959	18 −1 90 26 18 −45 −5 10 10	−2 1 12 1 2 −1 −1 0 −2	−4 14 −4 2 −7 2 5 0 5	2 2 2 1 1 1 −1 −1 −1
Σ35 7 1 1 80·959	30 −10 45 17 6 −90 2 11 10	0 0 −3 −1 5 −4 −1 0 1	−10 −10 −15 −8 −1 9 −3 4 −1	4 2 4 2 1 2 0 0 0
Σ35 9 0 1 64·623	33 −10 18 10 15 −90 2 10 17	−4 −1 1 1 5 2 −1 1 −1	1 5 29 −5 10 −5 −1 −5 6	−2 0 −1 3 3 2 0 0 −1
Σ35 9 0 5 88·363	10 −30 45 30 1 −54 5 6 26	−1 −3 −4 5 −1 1 0 −1 1	5 −10 15 −6 5 17 −1 −5 −3	−1 0 −4 1 1 2 0 0 0
Σ35 9 9 1 43·233	30 −1 54 10 30 −45 −5 6 26	1 1 5 −4 3 −1 −1 −1 0	6 −5 17 −5 10 15 −1 −5 3	1 1 3 0 0 −1 0 0 −1
Σ35 9 9 1 94·917	15 10 90 26 15 −54 −6 10 −1	−4 −4 3 5 −1 −1 0 1 1	5 −10 15 −3 13 19 −2 −3 1	−2 0 −1 1 −1 0 1 1 1
Σ35 9 9 4 88·363	10 −15 90 33 10 −18 −2 10 17	−2 1 5 −1 5 −1 −1 0 −1	5 −5 10 −1 29 5 −1 −6 5	1 1 1 −1 2 −1 −1 0 −1
Σ37 1 0 0 18·925	37 0 0 0 35 −36 0 4 35	1 0 0 0 1 18 0 −2 1	37 0 0 0 1 18 0 −2 1	0 0 0 0 1 6 0 −1 0
Σ37 1 1 2 91·549	0 −35 36 37 0 0 0 4 35	0 −1 −18 1 0 0 0 −2 1	−1 0 18 0 37 0 −2 0 −1	−1 0 −9 0 0 0 −1 0 0
Σ37 3 3 1 50·570	28 −12 63 21 28 −36 −4 7 28	3 4 3 −4 0 3 0 −1 1	7 −2 9 −4 17 16 −1 −5 4	3 3 2 0 0 0 0 0 0
Σ37 5 2 1 91·549	24 −8 81 28 3 −72 1 12 8	−2 −5 0 7 −1 1 0 0 1	13 −9 −2 9 8 10 −1 −5 3	−1 −2 −3 1 3 1 0 0 0
Σ37 7 3 1 84·572	28 −3 72 24 8 −81 −1 12 8	1 1 6 0 5 −2 −1 0 1	10 −8 9 −2 9 13 −3 −5 1	2 3 1 2 0 1 0 0 0
Σ37 9 0 1 43·136	36 −8 9 8 27 −72 1 8 28	−1 −4 3 1 3 5 −1 1 0	1 4 32 −8 5 3 −1 −4 5	0 −2 −1 1 1 4 0 0 0
Σ37 9 0 4 71·075	21 −28 36 28 12 −63 4 7 28	−1 −4 0 6 −1 4 −1 −1 1	4 12 13 −7 16 5 −1 −3 6	−2 −1 −1 2 1 4 0 0 0
Σ39 1 0 0 22·620	39 0 0 0 36 −45 0 5 36	1 0 0 0 −6 9 0 −3 −2	39 0 0 0 −6 9 0 −3 −2	0 0 0 0 1 1 0 −1 −1
Σ39 1 0 1 76·658	12 −36 27 36 9 −36 3 4 36	4 −5 1 3 6 0 0 0 1	9 −12 18 −12 3 15 −1 −3 −2	1 0 1 1 1 2 0 0 0
Σ39 3 1 0 76·658	36 9 36 9 12 −108 −4 12 9	−3 3 0 4 1 −4 −2 0 −1	9 −18 3 12 15 −9 −1 2 4	0 0 1 −1 2 0 −1 −1 0
Σ39 3 3 1 27·796	36 −9 36 12 36 −27 −3 4 36	0 3 6 1 4 −5 −1 0 0	12 −3 6 −9 12 15 −1 −3 6	1 1 2 1 0 1 0 0 0
Σ39 3 3 5 92·204	0 −36 45 39 0 0 0 5 36	0 6 −9 1 0 0 0 −3 −2	−9 0 6 0 39 0 −2 0 −3	−1 0 −1 0 0 0 −1 0 −1
Σ41 1 0 0 12·680	41 0 0 0 40 −27 0 3 40	1 0 0 0 1 13 0 −3 2	41 0 0 0 −13 1 0 −2 −3	0 0 0 1 1 1 −1 −1 −1
Σ41 1 1 0 55·877	32 9 72 9 32 −72 −8 8 23	−5 1 4 4 1 −4 −4 0 −1	4 −9 25 −4 9 16 −1 −8 4	2 1 −2 −1 0 2 −1 0 −2
Σ41 2 1 0 40·879	39 4 36 4 33 −72 −4 8 31	−1 2 4 2 1 −7 −2 0 −1	−1 −20 2 2 −1 37 −2 1 4	1 2 1 −1 −3 0 −1 −1 0
Σ41 3 0 1 55·877	32 −24 27 24 23 −72 3 8 32	0 5 3 −4 3 0 −1 −1 1	3 12 23 −8 9 7 −1 −4 6	3 4 3 1 1 0 0 0 0
Σ41 1 1 3 90·699	0 −40 27 41 0 0 0 3 40	0 −1 −13 1 0 0 0 −3 2	−1 0 14 0 41 0 −3 0 1	−1 −1 −1 0 0 0 −1 −1 −1

Table 1 (*cont.*)

System	ΣR	CSL	ΣDSC	Step vector	System	ΣR	CSL	ΣDSC	Step vector
Σ41 3 1 2 97·005	4 −33 72 39 −4 −36 4 8 31	1 −2 −7 2 1 4 0 −2 1	37 −2 1 2 1 20 −4 −2 1	0 −1 −4 1 1 2 0 −1 0	Σ45 9 6 1 86·177	30 6 99 30 15 −90 −5 14 6	1 −1 5 5 4 1 −1 1 0	6 −18 9 15 0 0 −1 3 6	1 1 0 3 3 2 0 0 0
Σ41 6 1 1 97·005	31 −12 72 24 −4 −99 4 13 4	−1 6 1 3 1 0 0 1 −2	5 −8 18 −12 11 6 −2 −5 1	1 2 0 0 1 0 −1 0 −1	Σ47 1 1 1 57·865	27 −34 54 38 27 −18 −2 6 43	−1 1 16 −1 3 5 −1 0 −2	−3 −17 −10 1 −10 19 −5 3 −1	8 8 7 3 3 3 −1 −1 −1
Σ41 7 5 1 90·699	24 4 99 31 12 −72 −4 13 4	1 0 3 6 1 −1 −1 2 0	6 −12 11 18 5 −8 −1 2 5	2 0 1 3 1 2 0 1 0	Σ47 2 0 1 43·664	38 −27 18 27 34 −54 2 6 43	3 −6 −1 1 13 −1 0 1 1	−10 −19 −1 −17 10 3 −3 −1 −5	−3 −1 −2 6 3 6 1 0 1
Σ41 9 9 5 61·601	24 −23 72 32 24 −27 −3 8 32	0 −7 −4 3 −2 0 −1 −1 1	8 −1 9 −3 26 12 −1 −5 4	−4 −3 −5 0 1 −1 0 0 0	Σ47 2 1 0 87·561	38 18 63 18 11 −126 7 14 2	−3 2 1 8 1 −3 4 0 1	−1 −8 16 2 16 15 −6 −1 2	1 1 0 0 0 0 1 −1 −1
Σ43 1 1 0 80·631	25 18 90 18 25 −90 −10 10 7	−9 1 2 9 1 −3 −5 0 −1	5 −9 19 −5 9 24 −2 −5 1	3 −3 −1 4 3 2 −2 −3 −2	Σ47 3 0 2 87·561	11 −42 54 42 2 −63 6 7 38	2 5 −2 −5 3 −3 0 1 1	6 −11 18 −7 5 26 −1 −6 −3	0 0 1 0 −1 −1 0 0 0
Σ43 2 1 0 27·905	42 2 27 2 39 −54 −3 6 38	3 2 4 −4 1 −6 −2 0 1	15 −13 −1 −13 26 2 −2 4 −3	3 3 2 −3 −3 −2 0 0 −1	Σ47 3 2 0 43·664	43 6 54 6 38 −81 −6 9 34	−3 −3 2 −2 7 −1 0 1 −2	15 −2 4 1 3 41 −1 −3 6	1 −1 −1 1 0 −1 0 0 0
Σ43 3 0 1 80·631	25 −30 54 30 7 −90 6 10 25	3 2 3 −5 3 0 −1 −1 1	3 15 19 5 18 3 −1 −5 8	3 3 3 2 −2 1 0 0 0	Σ47 5 1 3 97·949	6 −38 81 43 −6 −54 6 9 34	2 −4 −1 3 4 2 0 −1 2	44 −3 1 2 2 15 −3 −3 1	0 1 −1 1 1 3 0 0 1
Σ43 9 1 1 93·333	38 −9 54 18 −2 −117 3 14 2	1 −5 0 −3 1 3 −1 0 −2	−11 −6 16 −12 13 −6 −2 −5 −1	−2 −1 0 2 0 0 −1 −1 −1	Σ47 6 0 1 87·561	38 −21 54 21 2 −126 6 14 11	−2 1 5 −5 3 −2 −1 −1 −1	3 −16 25 −7 6 20 −2 −5 −1	1 1 0 −2 0 −1 −1 −1 −1
Σ43 9 9 2 60·766	30 −7 90 25 30 −54 −6 10 25	0 11 −3 3 1 −2 −1 1 −1	5 −3 18 −3 19 15 −1 −8 5	5 0 3 1 1 0 0 −1 0	Σ47 7 7 1 97·949	18 11 126 38 18 −63 −7 14 −2	−3 1 14 1 2 9 −1 0 −4	16 2 15 −8 −1 16 −1 −6 2	5 5 1 5 4 2 −2 −2 −1
Σ45 1 1 1 50·704	30 −30 45 33 30 −18 −2 5 42	−1 1 7 −1 4 −5 −1 −1 0	15 0 0 −6 9 18 −1 −6 3	3 1 0 −2 1 0 −1 −1 0	Σ47 9 9 1 37·073	42 −2 63 11 42 −54 −6 7 38	−3 5 5 −2 1 −2 1 −2 0	7 −5 19 −6 11 24 1 −6 4	0 0 4 −1 0 −1 −1 0 −1
Σ45 2 1 0 48·190	42 6 45 6 33 −90 −5 10 30	0 2 3 0 1 −6 −3 0 −1	9 −3 18 −18 6 9 0 −5 0	1 1 2 0 0 −2 0 0 −1	Σ47 9 9 2 86·340	21 −2 126 38 21 −54 −6 14 11	2 10 5 −5 10 2 −1 −3 −1	7 −6 13 3 16 28 −2 −5 3	3 7 3 −1 4 0 −1 −2 −1
Σ45 2 1 1 86·177	15 −30 90 42 6 −45 2 11 30	−2 −3 −2 −1 −9 5 −1 1 0	−15 0 0 3 −9 18 −2 6 3	0 −1 −2 0 −2 −4 0 0 0	Σ49 2 2 1 49·227	36 −23 72 31 36 −36 −4 8 41	−1 1 26 0 2 9 −1 0 −3	9 4 18 20 −2 −9 −1 5 −2	6 6 5 3 3 3 −1 −1 −1
Σ45 3 0 2 48·190	33 −30 18 30 30 −45 2 5 42	1 −4 −1 1 −1 8 −1 −1 1	6 12 9 −15 15 0 −1 −2 6	−1 −1 −1 3 1 1 0 0 −1	Σ49 3 2 0 62·005	41 12 72 12 31 −108 −8 12 23	−3 −2 3 −2 3 −4 0 −2 −1	45 −2 3 6 3 20 −4 −2 3	−1 −2 1 −1 1 −1 0 −1 −1
Σ45 3 3 2 78·463	15 −30 90 42 15 −18 −2 10 33	−1 1 7 1 5 −4 −1 0 −1	15 −15 0 −3 −6 18 −2 −4 −3	0 1 3 1 2 0 0 0 −1	Σ49 4 1 0 49·227	48 4 27 4 33 −108 −3 12 32	1 4 2 −1 1 −5 −2 0 1	16 −1 18 −15 4 26 −1 −3 5	1 1 2 −2 0 −2 0 0 0
Σ45 6 0 1 48·190	42 −15 18 15 30 −90 2 10 33	−1 −4 5 1 7 1 −1 1 0	3 −18 6 −15 0 15 −2 −3 −4	−1 −1 2 4 4 1 0 0 0	Σ49 3 3 1 43·574	40 −15 72 24 40 −45 −5 8 40	3 −3 5 −5 −3 0 0 −1 −1	8 −1 17 −5 19 20 −1 −6 4	2 2 2 −3 −3 −4 −1 −1 1
Σ45 6 3 1 78·463	33 −6 90 30 15 −90 −2 14 15	−1 5 4 2 5 −2 −1 0 −1	9 −6 18 0 15 0 −6 −1 3	2 3 3 2 3 2 0 −1 0	Σ49 9 0 2 62·005	41 −24 36 24 23 −108 4 12 31	3 0 −2 1 3 6 0 −2 1	2 12 33 −6 13 −1 −1 −6 8	0 0 1 4 2 1 0 −1 0
Σ45 9 3 1 50·704	42 −6 45 15 30 −90 −2 11 30	1 −5 4 2 2 5 −1 0 1	−3 −18 9 15 0 0 −2 3 6	−1 0 0 1 4 1 0 0 0	Σ49 9 0 5 72·174	24 −40 45 40 15 −72 5 8 40	5 8 0 −3 15 54 0 2 1	5 −19 20 −8 1 17 −1 −6 −4	3 3 4 7 6 7 1 1 1
Σ45 9 3 2 86·177	30 −15 90 33 6 −90 2 14 15	2 5 2 −4 5 −1 −1 0 1	15 −15 0 12 6 9 −2 −1 6	1 2 2 1 −2 2 0 0 0	Σ49 9 9 4 72·174	24 −23 108 41 24 −36 −4 12 31	−3 1 6 0 3 −2 −2 0 −1	6 −1 13 −2 33 12 −1 −8 6	3 1 0 0 1 0 −1 0 −1

ratios considered in this study.* Considerations of the symmetry of the tetragonal lattice (Grimmer, 1980) limit the value of θ to 98·4°. All the vectors in the table are listed columnwise, with the three columns of step vectors corresponding respectively to the columns of the DSC vectors. For the [001] misorientation axis, our results are identical to those obtained by King (1982) for the cubic system. For irrational values of the parameter τ in (21), coincidence orientations are possible only about this axis. The $\Sigma = 5$ geometry is shown in Fig. 1, for a rotation of 36·87° about the [001] axis.

The (110) and the $(1\bar{1}0)$ twin boundaries in $YBa_2Cu_3O_{7-\delta}$ can be considered as CSL-related

* Lists of Σ values, axes, angles, CSL's, DSC's and step vectors for the axial ratios 15:15:136, 6:6:55, 15:15:138 and 15:15:140 have been deposited with the British Library Document Supply Centre as Supplementary Publication No. SUP 52341 (8 pp.). Copies may be obtained through The Executive Secretary, International Union of Crystallography, 5 Abbey Square, Chester CH1 2HU, England.

boundaries, with a rotation angle of 90° about the [001] axis. The Σ value can be obtained quite trivially as 1.

The choice of axes within the standard stereographic triangle can be limited by the considerations of lattice symmetry and equivalent rotations, as shown by Grimmer (1980). It is interesting to note that the choice of the axial ratio 1:1:9 yields a value of $\Sigma = 3$ for a rotation of 90° about the [100] axis. We consider this geometry (Fig. 2) to be a peculiarity of this axial ratio. The values of Σ for rotations about the [331] axis are three times the values of Σ for rotations about the [111] axis for cubic crystals, for the same rotation angle. The pseudo-equivalence of these axes is illustrated in Fig. 3. The Cu atoms located at the corners of the three perovskite cubes, which are stacked to form the $YBa_2Cu_3O_{7-\delta}$ cell, form a distorted cubic pseudo-lattice, which could form the basis for CSL's. Translations by the DSC vectors associated with these CSL's, however, would not conserve the grain-boundary structure unless they were equal to the 'true' DSC vectors determined here. Fig. 4 shows a $\Sigma = 13$ geometry, for a rotation of 67·38° about the [100] axis for an axial ratio of 1:1:9. Our results are identical to those obtained from the geometrical construction.

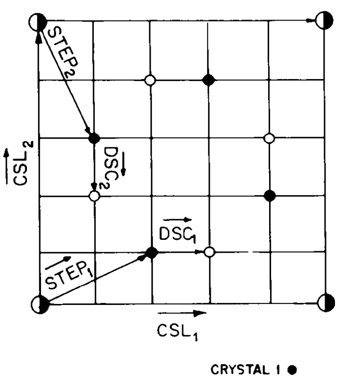

Fig. 1. Examples of CSL, DSC and step vectors for the $\Sigma5$, 36·87°/[001] coincidence system.

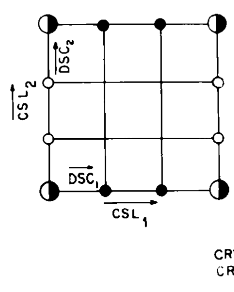

Fig. 2. Examples of CSL, DSC and step vectors for the $\Sigma3$, 90°/[100] coincidence system.

As can be seen from Fig. 5, the distribution of CSL's in misorientation space is intermediate, in the sense that it falls in between those for hexagonal (which form dense clusters) and cubic (which are widely spaced). The existence of clusters would imply the possibility of structural transformations as a function of misorientation, temperature or composition, in which the grain-boundary structure could change from one CSL-related structure to another.

No coincidence rotations are obtained for axial ratios of 15:15:137 and 15:15:139 about axes other than [001]. The possibility of the existence of coinci-

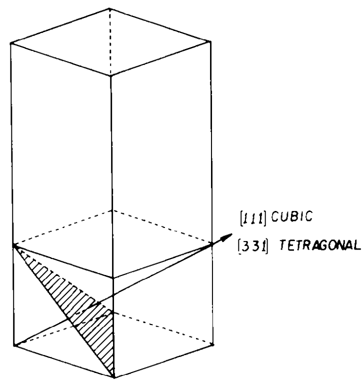

Fig. 3. Pseudo-equivalence of [111]/cubic and [331]/tetragonal axes.

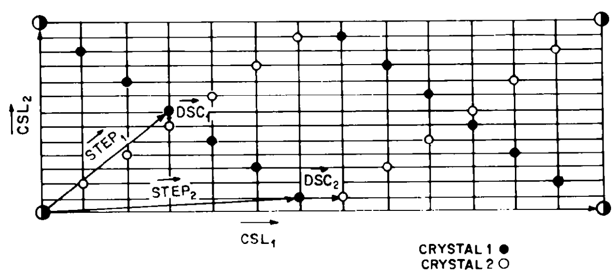

Fig. 4. Examples of CSL, DSC and step vectors for the $\Sigma13$, 67·38°/[100] coincidence stystem.

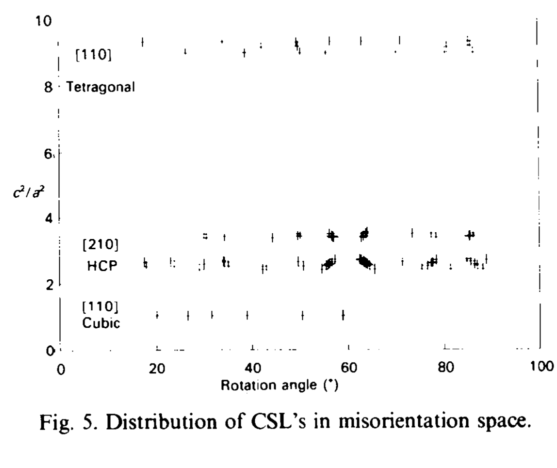

Fig. 5. Distribution of CSL's in misorientation space.

dent grain boundaries with $\Sigma > 50$ cannot be ruled out, but such high values of Σ are of little or no physical significance. The axial ratios considered in this work, though they are approximations to the true $YBa_2Cu_3O_{7-\delta}$ structure, yield useful criteria for characterizing grain boundaries. Chisholm & Smith (1989), Babcock & Larbalestier (1989) and Babcock (1988) have observed grain-boundary-dislocation networks. Babcock (1988) has speculated on the possibility of these structures being related to CSL structures.

Concluding remarks

Consideration of the geometrical structure of grain boundaries can provide a valuable insight into the properties of materials. We have presented here a method to determine the geometry of grain boundaries in tetragonal and near-tetragonal orthorhombic crystal systems, with particular emphasis on $YBa_2Cu_3O_{7-\delta}$. Data on the possible grain-boundary structures of $YBa_2Cu_3O_{7-\delta}$ are presented. It is hoped that this will aid in characterizing the grain-boundary structures observed in $YBa_2Cu_3O_{7-\delta}$.

This work was supported by the National Science Foundation, under grant No. DMR-8901994. NC also received support from the US Department of Energy, through contract No. DE-AC-87CH00016. We would like to thank the referees for many helpful suggestions, and for drawing our attention to the work of Grimmer and Erochine *et al.*

References

Babcock, S. E. (1988). *EMSA Proc.* pp. 622–623.
Babcock, S. E. & Larbalestier, D. C. (1989). *J. Mater. Res.* Submitted.
Bonnet, R. (1981). *Acta Cryst.* **A27**, 184–189.
Chen, F. R. & King, A. H. (1987). *Acta Cryst.* **B43**, 416–422.
Chen, F. R. & King, A. H. (1988). *Philos. Mag. A*, **57**, 431–455.
Chisholm, M. F. & Smith, D. A. (1989). *Philos. Mag. A*, **59**(2), 181–197.
Erochine, S. & Nouet, G. (1983). *Scr. Metall.* **17**, 1069–1072.
Grimmer, H. (1980). *Acta Cryst.* **A36**, 382–389.
Grimmer, H. & Warrington, D. H. (1987). *Acta Cryst.* **A43**, 232–243.
Johnston, D. C. (1987). *Chemistry of High Temperature Superconductors*, ACS Symposium Series 351, pp. 136–151. Washington, DC: American Chemical Society.
King, A. H. (1982). *Acta Metall.* **30**, 419–427.
King, A. H. & Smith, D. A. (1980). *Acta Cryst.* **A36**, 335–343.

Acta Cryst. (1990). **B46**, 125–131

Structural Study of the Phase Transition of $Na_4Ca_4[Si_6O_{18}]$

By Hitoshi Ohsato* and Yoshio Takéuchi

Mineralogical Institute, Faculty of Science, University of Tokyo, Hongo, Tokyo 113, *Japan*

and Iwao Maki

Department of Materials Science and Engineering, Nagoya Institute of Technology, Gokiso-cho, Showa-ku, Nagoya 466, *Japan*

(*Received* 30 *June* 1989; *accepted* 26 *September* 1989)

Abstract

The structure of $Na_4Ca_4[Si_6O_{18}]$, which undergoes a reversible phase transition at 748 K, has been studied by means of X-ray single-crystal diffraction at 993, 888, 773, 738, 643 and 523 K. The crystal data of the high-temperature modification at 773 K are: $M_r = 708{\cdot}8$, trigonal, $R\bar{3}m$, $a_R = 7{\cdot}519$ Å, $\alpha = 89{\cdot}22°$, $Z = 1$; $a_H = 10{\cdot}561\,(1)$, $c_H = 13{\cdot}199\,(3)$ Å, $V_H = 1274{\cdot}9$ Å^3, $Z = 3$, $D_x = 2{\cdot}77$ Mg m^{-3}, λ(Mo $K\alpha$) = 0·71073 Å, $\mu = 1{\cdot}89$ mm^{-1}, $F(000) = 1056$, $R = 0{\cdot}047$ for 599 observed reflections ($F_{obs} > 3\sigma$). The high-temperature form, made up of puckered six-membered $[Si_6O_{18}]^{12-}$ rings, is isostructural with $Na_6Ca_3[Si_6O_{18}]$. One of the cation sites is only partly occupied by Na ions with the remainder vacant. In the low-temperature form the vacancies are clustered to produce a specific vacant cation site. The vacancies, in both forms, can accommodate additional Na ions with the replacement of Ca by 2Na and thus play an essential role in the formation of continuous solid solutions as represented by $Na_{4+2x}Ca_{4-x}[Si_6O_{18}]$ $(0 \le x \le 1)$. The difference in structure between the high- and low-temperature forms is described in terms of their cation coordination polyhedra and configurations of the $[Si_6O_{18}]^{12-}$ ring.

* Present address: Department of Materials Science and Engineering, Nagoya Institute of Technology, Gokiso-cho, Showa-ku, Nagoya 466, Japan.

0108-7681/90/020125-07$03.00